Mesenchymal Stem Cells Expressing Osteogenic and Angiogenic Factors Synergistically Enhance Bone Formation in a Mouse Model of Segmental Bone Defect

Sanjay Kumar[1], Chao Wan[1], Girish Ramaswamy[2], Thomas L Clemens[1] and Selvarangan Ponnazhagan[1]

[1]Department of Pathology, The University of Alabama at Birmingham, Birmingham, Alabama, USA; [2]Department of Biomedical Engineering, The University of Alabama at Birmingham, Birmingham, Alabama, USA

The potential of mesenchymal stem cells (MSC) in tissue regeneration is increasingly gaining attention. There is now accumulating evidence that MSC make an important contribution to postnatal vasculogenesis. During bone development and fracture healing, vascularization is observed before bone formation. The present study determined the potential of MSC, transduced *ex vivo* with a recombinant adeno-associated virus 6 (rAAV6) encoding bone morphogenetic protein 2 (BMP2) and vascular endothelial growth factor (VEGF) in a mouse model of segmental bone defect created in the tibiae of athymic nude mice. Mouse MSC that were mock-transduced or transduced with rAAV6-BMP2:VEGF were systemically transplanted following radiographic confirmation of the osteotomy. Effects of the therapy were determined by enzyme-linked immunosorbent assay measurements for BMP2 and VEGF, dual-energy X-ray absorptiometry (DXA) for bone density, three-dimensional microcomputed tomography (μCT) for bone and capillary architecture, and histomorphometry for bone remodeling. Results of these analyses indicated enhanced bone formation in the group that received BMP2+VEGF-expressing MSC compared to other groups. The therapeutic effects were accompanied by increased vascularity and osteoblastogenesis, indicating its potential for effective use while treating difficult nonunion bone defects in humans.

Received 25 May 2009; accepted 20 December 2009; published online 12 January 2010. doi:10.1038/mt.2009.315

INTRODUCTION

Among millions of fractures suffered annually in the United States, 5–10% of these result in impaired healing, including nonunions.[1] In most of these cases, bone regeneration needs to be enhanced for healing, and the failure to do so results in severe lifestyle impairment. Bone marrow-derived mesenchymal stem cells (MSC) have been demonstrated to be an attractive therapeutic cell source for tissue regeneration and repair. In recent years, gene transfer has emerged as an effective approach to deliver therapeutic proteins in a more physiological and persistent manner.[2–4] Bone is a highly vascularized tissue, and angiogenesis plays an important role in bone growth and remodeling.[5,6] Vascular endothelial growth factor (VEGF) is a potent angiogenic factor that is shown to be essential in the bone repair for both intramembraneous[7] and endochondral bone formation.[7,8] Bone morphogenetic proteins (BMPs) are a well-characterized growth factor and have been investigated for their capacity to improve bone healing. Among BMPs, BMP2 is an osteogenic growth factor commonly used in both ectopic and orthotopic sites for bone generation.[9,10] It has been successfully tested in fracture sites in rats,[11] rabbits,[12,13] and dogs.[14] However, there is concern that just a one-time exposure to an exogenous growth factor may not induce adequate osteogenic signal in many clinical situations where there is only limited bone-healing potential, which is due to compromised vascularity, limited bone stock, and abundant fibrous tissue.[15] Recent work by Patel *et al.*[16] demonstrated that dual delivery of angiogenic and osteogenic growth factors by gelatin microparticles, when incorporated within the scaffold pores, improved blood-vessel formation and bone growth, which in turn suggests an interplay between these growth factors for early bone regeneration. Studies have also demonstrated the importance of supplying extra VEGF for bone formation induced by osteogenic BMPs.[17] VEGF, in addition to its role in cartilage resorption during endochondral bone formation,[18] influences other steps in bone formation and bone-healing processes. As BMP2 and VEGF are involved in bone formation via different pathways, it is possible to attain a synergistic response of bone regeneration than with a single factor alone during the early stages of fracture healing. We hypothesized that MSC, modified to express both BMP2 and VEGF, can be used for controlled delivery of angiogenic and osteogenic factors and can mimic natural bone healing to promote bone regeneration in segmental defect. Using an *ex vivo* approach with genetically engineered MSC to express BMP2 and VEGF, the present study demonstrates that transplantation of MSC, expressing both BMP2 and VEGF, in a mouse segmental defect resulted in efficient bone formation that correlated with increased vascularity.

Correspondence: *Selvarangan Ponnazhagan, Department of Pathology, 19th Street South, University of Alabama at Birmingham, Birmingham, AL 35294-0007, USA. E-mail: pons@uab.edu*

RESULTS

MSC phenotyping and expansion of luciferase-expressing MSC for cell tracking

MSC were isolated from the bone marrow and cultured *in vitro*. The cultured cells appeared to form a morphologically homogeneous population of fibroblast-like cells and were confirmed by flow cytometry analysis as positive for CD105, CD73, CD44, CD29, and *Sca*I. The cells were also negative for CD45, CD34, and CD31. To track the marked MSC *in vivo* after systemic transplantation, luciferase-expressing MSC were isolated from a luciferase-transgenic mouse, and a transgene expression from the MSC was confirmed in a Berthold SIRIUS luminometer (Pforzheim, Germany). Before testing MSC *in vivo* their stem cell plasticity was confirmed by differentiating them into osteoblast, adipocyte, chondrocyte, and myocyte lineages as described earlier.[19]

Expression of BMP2 and VEGF from transduced MSC, and transplantation into mice with osteotomy

Culture-expanded MSC were mock-transduced or transduced with recombinant adeno-associated virus 6 (rAAV6)-BMP2:VEGF, and culture supernatants were used to determine the expression level of BMP2 and VEGF by enzyme-linked immunosorbent assay. Results indicated the secretion of BMP2 in transduced MSC was at the level of 41 ± 7 ng/10^6 cells and VEGF at the level of 7.5 ± 1.2 ng/10^6 cells. MSC were transduced with AAV-green fluorescent protein (GFP) control vector to normalize the basal levels of VEGF and BMP2 secretion. Transplantation of MSC, secreting dual-growth factors, showed augmented bone healing in the BMP2:VEGF group as monitored by X-ray image and dual-energy X-ray absorptiometry (DXA) analyses in mice with osteotomy (**Figure 1a–c**).

Homing of systemically transplanted MSC to the fracture site

To investigate the homing of systemically transplanted MSC *in vivo*, the cells were intravenously injected (2×10^5 cells/mouse) after surgically creating a 2–3-mm segmental defect in right tibiae of mice. Bioluminescence imaging, performed after 24 hours of MSC transplantation, shown in **Figure 2a**, indicated the homing pattern of MSC upon *in vivo* administration. Initially, most of the cells were trapped in the lungs and liver, in addition to significant number of MSC in the region of osteotomy in the tibia; however, with time, injected MSC were cleared from lung, liver, and other tissues, as shown in **Figure 2b** and **Supplementary Figure 1b,c**. Other factors such as bioluminescence imaging and quantification of luciferase signal and immunohistochemistry with luciferase antibody in organs harvested from MSC-transplanted mice also confirmed this effect (**Supplementary Figure 1a–c**). Total body X-ray analysis, performed 5 weeks after MSC transplantation, indicated no unintended ossification in other soft tissues (**Supplementary Figure S2**).

VEGF-enhanced neoangiogenesis resulted in proper vasculature around the segmental defect area

For quantification of angiogenic response in the MSC-transplanted mice, the procedure of microcomputed tomography (μCT)-based angiography using microfil was performed at week 5. Results of this experiment, as shown in **Figure 3a**, indicated several new sprouting blood vessels, which were spread around the segmental defect area in the BMP2:VEGF group compared to other MSC-injected group, where vessels numbers were low and vessels not

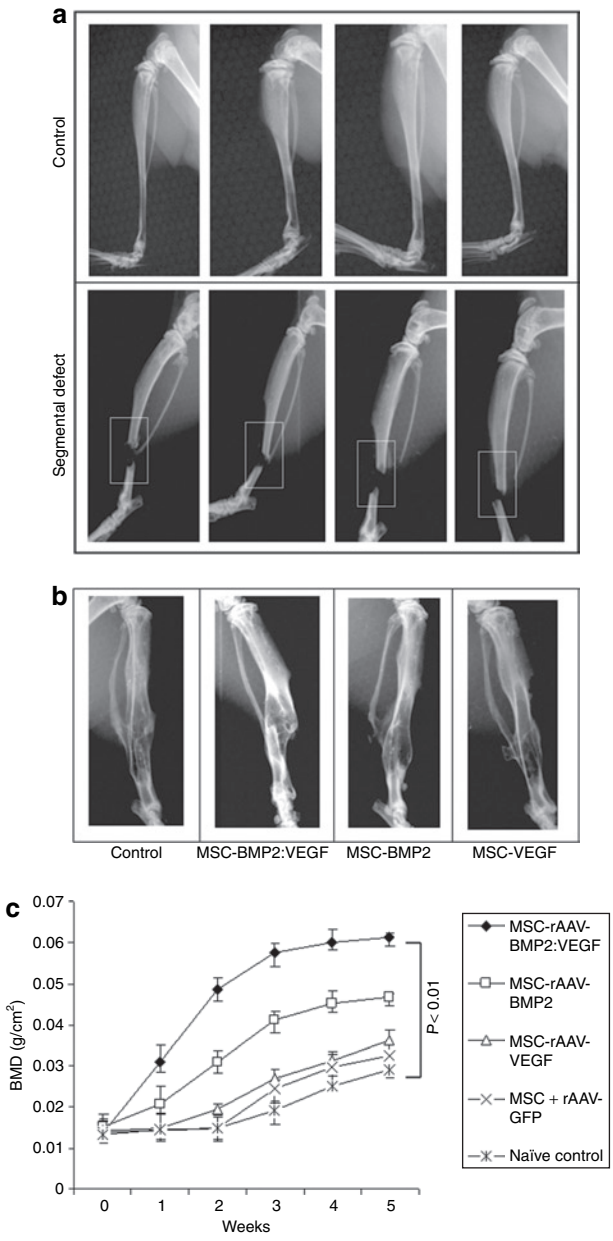

Figure 1 Bone mineral density (BMD) in the segmental defect area of tibiae during fracture healing. (**a**) Segmental defect was surgically created in the right tibia of 10–12-week-old nude mice. (**b**) X-ray imaging of mice after 5 weeks of MSC transplantation showing the fracture healing process. (**c**) A total of 1×10^6 MSC that were unmodified, transduced with rAAV6-BMP2:VEGF or rAAV6-GFP, were administered in five consecutive days by intravenous injection. Mice were anesthetized with isoflurane for dual-energy X-ray absorptiometry (DXA) analysis. BMD was determined weekly around the fractured area of tibia by noninvasive DXA to follow the bone growth. DXA was performed in a GE Lunar PIXImus machine, and data analyses were performed using PIXImus software version 1.43.020. BMP2, bone morphogenetic protein 2; MSC, mesenchymal stem cells; rAAV, recombinant adeno-associated virus; VEGF, vascular endothelial growth factor.

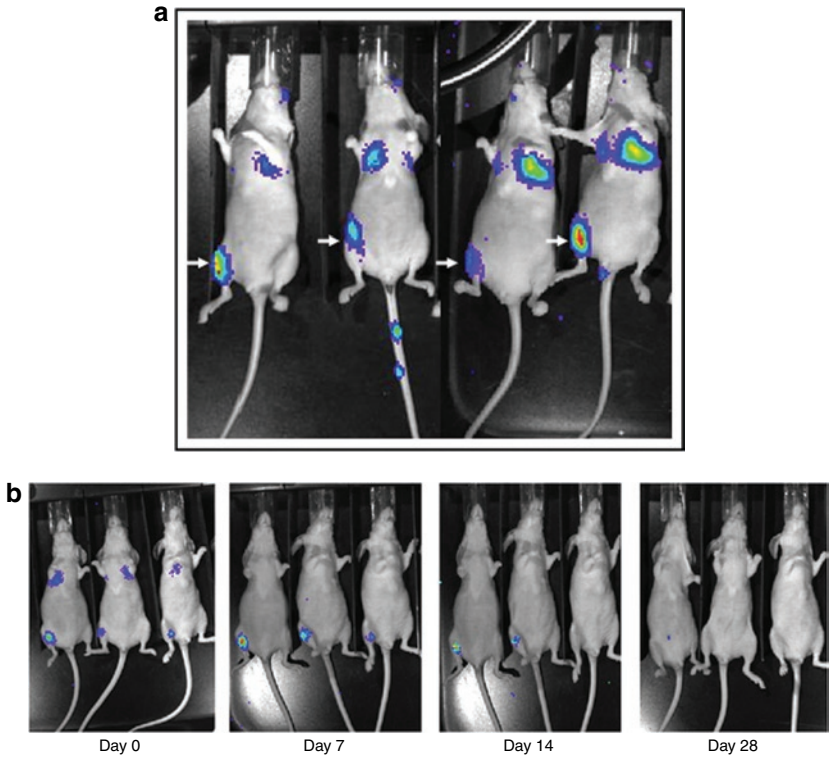

Figure 2 Biodistribution of systemically transplanted luciferase-positive MSC. (**a**) Luciferase-positive MSCs were intravenously transplanted into nude mice, following creation of tibial segmental defect in the right leg, and bioluminescence image was monitored after 24 hours. Representative images of mice showing homing-in-on of transplanted MSC to the site of segmental defect are shown above. (**b**) Bioluminescence imaging was performed at indicated time points to track long-term viability and existence of transplanted, luciferase-positive MSC in recipient mice. MSC, mesenchymal stem cells.

well spread out. This suggests that growth factors released from the MSC in response to local stimuli did not fall below the critical physiological levels during the early fracture-healing process because blood vessel network was stable and consistent during the process of remodeling till 5 weeks. Microarchitectural parameters, shown in **Figure 3b** also corroborated increased vessel number and vessel connectivity density in BMP2:VEGF group compared to control groups ($P < 0.03$).

VEGF expression synergistically enhanced bone formation with BMP2

Noninvasive X-ray imaging of fractured tibia after 5 weeks indicated a robust bone growth around the fracture area in BMP2:VEGF group (**Figure 1b**). Cohorts of mice were evaluated for bone formation in the tibia around the fractured area by noninvasive DXA analysis. Results of DXA analysis of bone growth around the segmental defect area (see **Figure 1c**) indicated a gradual increase in bone density in all MSC-injected mice, but the group receiving BMP2 and VEGF had the highest bone growth compared to others. In addition, µCT analysis after week 5 reconfirmed the DXA finding, that the dual-therapy promoted highest bone regeneration. Bone formation was observed to be the least in the control and VEGF groups. To quantify the new bone growth as measured by microarchitectural parameters such as trabecular bone volume/tissue volume, trabecular connectivity density, trabecular number and trabecular thickness, and trabecular bone and cortical bone, µCT analysis was performed around the fracture area after 5 weeks of MSC therapy. Results of this analysis also corroborated with highest therapy effects on all these parameters in the group receiving MSC, expressing BMP2 and VEGF (**Figure 4a,b**).

VEGF increased bone mineral density and bone mineral content by increasing cell recruitment

End-point µCT analysis of healed bones (see **Figure 5**) indicated the benefit of transplanting MSC-expressing BMP2 and VEGF on bone growth. Tibial bone defect was corrected with new bone growth leading to less deformed skeletal integrity compared to control tibiae, where callus was inflated due to inefficient bone-healing process. Histology of the healing area (see **Figure 6a**) indicated most efficient bone growth in the BMP2:VEGF group compared to other MSC administered groups. This group also had densely packed bone marrow with abundant marrow cells than other groups (**Figure 6a**).

Combination therapy increases the biomechanical quality of the bone

To assess the biomechanical quality of new bone growth following the MSC therapy of segmental defect in mice, tibiae were isolated from mice after 16 weeks of therapy and subjected to three-point bending test. Results as shown in **Figure 6b** demonstrated a significant increase in peak load, stiffness, and toughness of tibial bones in the dual-therapy group, compared to other MSC-injected groups ($P < 0.05$), and this increase in bone quality was

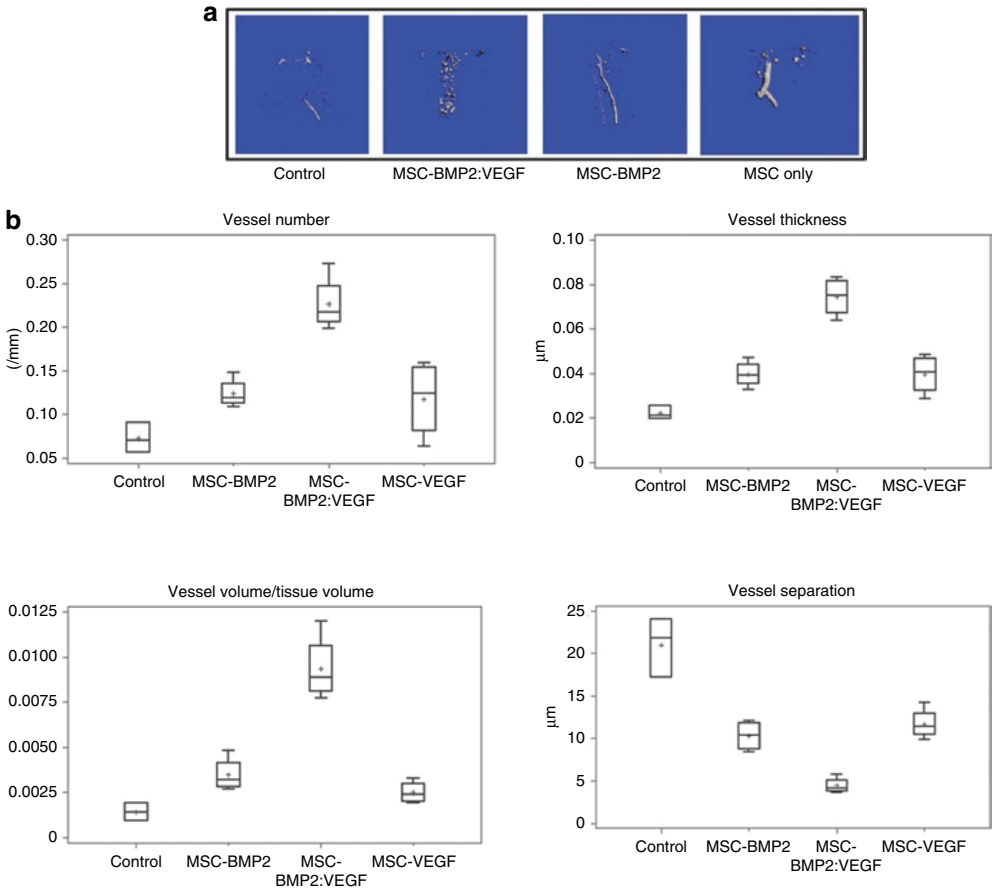

Figure 3 MSC-expressing osteogenic and angiogenic factors show vascularized bone development around segmental defect area of tibia and microarchitectural parameters of Microfil-perfused vasculature of tibia. (**a**) After intravenous transplantation of MSC, mice were sacrificed after Microfil perfusion from each group, and bones were used for µCT. Representative µCT images of vasculature in Microfil-perfused tibia (around the segmental defect area) show three-dimensional image of region of interest (ROI) extracted from reconstructed vasculature volume after 5 weeks of treatment of mice in control group; those injected with MSC-expressing BMP2 and VEGF, those injected with MSC-expressing BMP2, and those injected with MSC-expressing VEGF are shown. (**b**) Denoted values of microarchitectural parameters were determined from three-dimensional µCT measurements from groups of mice receiving AAV-BMP2:VEGF treatment or no treatment. Horizontal lines in each box from top to bottom indicate 25th, 50th, and 75th percentiles. Error bars indicate 10th and 90th percentiles. AAV, adeno-associated virus; BMP2, bone morphogenetic protein 2; µCT, microcomputed tomography; MSC, mesenchymal stem cells; VEGF, vascular endothelial growth factor.

the result of a delivery of both growth factors, BMP2 and VEGF, as a single-growth factor was not sufficient to attain comparable bone growth and biomechanical properties.

DISCUSSION

MSC are nonhematopoietic adult stem cells with broad differentiation potential and, hence, are regarded as possible effectors for tissue repair *in vivo*. For most therapeutic purposes, systemic infusion of MSC remains the practical mode of administration. However, this also requires that MSC must be capable of migrating and homing in on to the targeted tissue upon systemic delivery. We are still in the process of learning about the cellular cues that enable MSC to be directed to the site of tissue damage and the mechanisms by which MSC then exert therapeutic effect. What limit the homing in, and engraftment, on MSC *in vivo* is unclear, and the exact molecular mechanisms underlying MSC homing also remain undefined thus far. However, use of ectopic homing signal α4β1-integrin on MSC increased the bone-homing potential of these cells, as observed in our earlier studies.[19] The objective of the present study was that osteogenic response by osteoinductive factors would be augmented with concomitant induction of vascular network by the angiogenic factor VEGF, and this would facilitate proper nutrient supply required for the migration and recruitment of cells necessary to support bone-forming osteoprogenitors. Fracture healing is a complex physiological process that involves an orchestrated series of cellular events.[20] Molecular mechanisms governing therapeutic effects of MSC are not well elucidated. However, it is attributed to a large number of potent mediators secreted from MSC in response to surrounding local stimuli that would potentially be more relevant to MSC therapeutic properties than transdifferentiation of MSC into homed tissue. In our transplantation model, MSC were not found to be integrated into newly formed bone but were present in a supportive role during early bone formation. MSC express high levels of growth factors such as hepatocyte growth factor, transforming growth factor, fibroblast growth factor-2 (FGF2), VEGF, matrix metalloproteinase-2, and matrix metalloproteinase-9, which may be involved to a certain extent in MSC-induced therapeutic response.

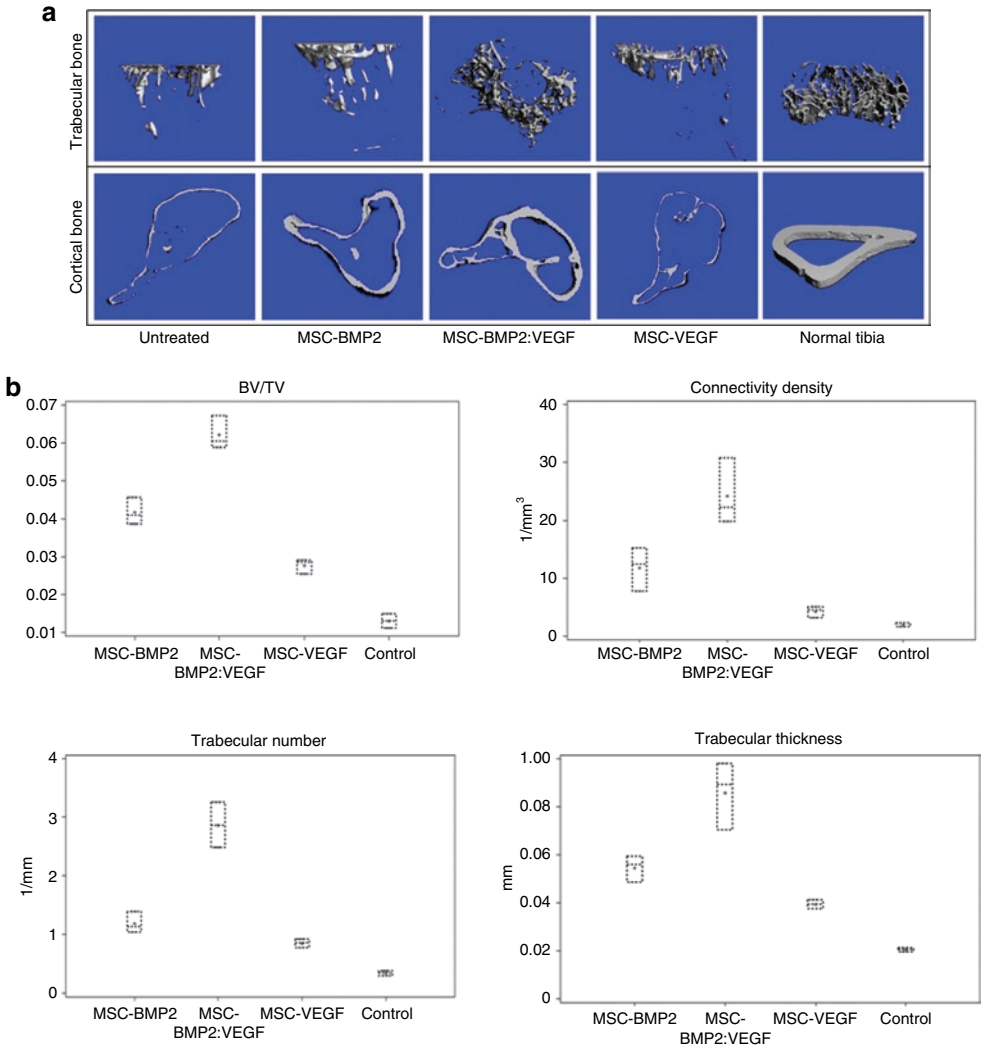

Figure 4 μCT analysis of cortical and trabecular bones of fractured tibia and microarchitectural parameters of trabecular bone around the fractured tibia after MSC therapy. (**a**) Tibia from MSC-transplanted cohorts of mice were used for μCT analysis of cortical bone and trabecular bones. Representative images from indicated groups show three-dimensional images of tibia extracted from reconstructed bone volume, 8 weeks after treatments. (**b**) Denoted values of microarchitectural parameters were determined from three-dimensional μCT measurements from groups of mice receiving indicated treatments or no treatment (control). Horizontal lines in each box from top to bottom indicate 25th, 50th, and 75th percentiles. Error bars indicate 10th and 90th percentiles. BMP2, bone morphogenetic protein 2; μCT, microcomputed tomography; MSC, mesenchymal stem cells; VEGF, vascular endothelial growth factor.

The use of luciferase-marked cells to track the homing and engraftment indicated that, upon intravenous administration of MSC, the cells homed in on to other organs, in addition to the fracture site, but luciferase signal from these nonspecifically homed organs became undetectable after 1 week of transplantation, possibly because these organs are not the natural niche for MSC. The gradual decrease of transplanted MSC over time also corroborates our previous studies.[21] These analyses indicate that therapeutic effects observed in this study may also be due to the recruitment of endogenous bone progenitors stimulated by BMP2 and VEGF and other growth factors/cytokines expressed by transplanted MSC during the initial phase of bone healing. Bone regeneration requires co-operation and contribution from resident bone cells and components of bone marrow and thus leading to the development of proper vascular network around the injury, which will facilitate recruitment of osteoprogenitor cells for bone development. After transplantation, the transplanted MSC, expressing BMP2 and VEGF, possibly remained as a potential source for necessary growth factors and cytokines required for bone regeneration. The beneficial effects of MSC might be mediated, at least in part, by their ability to supply required amount of both angiogenic and osteogenic. Whether MSC that homed in on to regions other than the fracture site contributed to therapeutic effects by paracrine mechanism needs to be determined.

The use of synthetic radiopaque agent Microfil at an early time point allowed visualization and quantification of the vasculature, which showed dual therapy with BMP2 and VEGF had significant effect on neoangiogenesis with even distribution of blood vessels around the healing area with uniform vascular diameter and size. Vascularization is observed at the transition of preosteoblast to mature osteoblasts during both bone development and fracture healing. This suggests the effect of growth factors

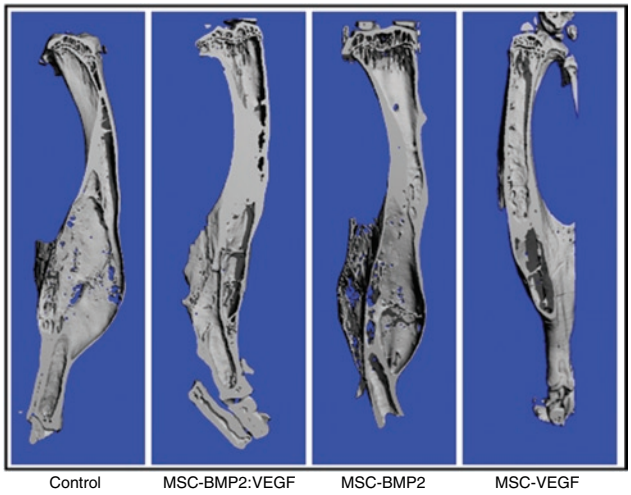

Figure 5 μCT analysis of fixed tibia after MSC therapy. Tibiae from MSC-transplanted cohorts of mice were used for μCT analysis. Representative images from indicated groups show three-dimensional images of tibiae extracted from reconstructed bone volume, 16 weeks after the treatment. BMP2, bone morphogenetic protein 2; μCT, micro-computed tomography; MSC, mesenchymal stem cells; VEGF, vascular endothelial growth factor.

during dynamic interaction between several cell types in the bone marrow. Interpretation of synergistic increase in bone regeneration results also necessitates careful considerations, as BMP2 and VEGF can have multiple effects on different cell types, and what role each growth factors have during the process of bone healing needs to be further investigated. VEGF may cause proliferation and migration of endothelial cells, promote chemotaxis,[22–24] and influence osteoblast differentiation.[25–27] Similarly, BMP2 also has several important functions driving osteoprogenitor cell proliferation and differentiation and can, at the same time, play an indirect role in stimulating osteoblast production of VEGF[28] and also engaging endothelial cells by chemotaxis.[29] Increased bone volume and number of bone marrow cells in the dual therapy group suggests that increased vascularity during the bone-healing process may have resulted from continuous flow of all the necessary nutrients and cells needed for bone regeneration. The difficulty in interpretation of their role could be linked to the diversity of cells recruited *in situ* around the fracture area and to the elusive nature of the paracrine signals that are exchanged between the MSC and cells involved in fracture repair, for example, endothelial, osteoprogenitor, and stromal cells. Bone marrow–recruited pericytes have a major role during elongation, vessel maturation, and vascular remodeling.[30,31] Furthermore, pericyte density was shown to have an impact on vessel morphology, which occurs in response to VEGF.[32,33] Thus, MSC could facilitate the anchoring, maintenance, organization, and differentiation of endothelial cells into stable vascular structures because MSC also express immature pericyte markers.[34] MSC being an integral component of bone marrow stromal system also shows a marked degree of phenotypic plasticity; a specific example is the ability to manipulate MSC in culture to differentiate into either adipocyte or chondrocyte and then subsequently "regress" the cells and direct them along the osteogenic pathways.[35] Although generally a 2–3-mm-long segmental defect usually fails to heal, in our study, we observed modest bone growth in control mice also. This is possibly because mice used in our study were relatively of younger age. Evidence in recent literature also suggests that influence of age on MSC number and proliferation capabilities are at peak during young age but gradually decrease with age. It remains possible, however, to further improve the therapy effects by using other proangiogenic signals such as FGF and hypoxia-inducible factor-1α. In this study, FGF was not chosen despite its potential in inducing more mature vessels because, at low concentrations, FGF arrests the differentiation of MSC but maintains the stem cells in a pluoripotent state.[36] In addition, the effects of this therapy could be maximized by local injection of modified MSC at the fracture site in situations where the defect is restricted to a specific region.

Overall, the present study demonstrates the potential of MSC-expressing BMP2 and VEGF in order to enhance bone healing in segmental defect. Future evaluation of this strategy in multiple fracture and nonunion fracture models should increase the potential of this approach for clinical use.

MATERIAL AND METHODS

Cells and reagents. Human embryonic kidney-293 cell line was purchased from American Type Culture Collection (Manassas, VA) and maintained in Dulbecco's modified Eagle's medium supplemented with 10% newborn calf serum. Restriction endonucleases and other modifying enzymes were purchased from either NEB (Beverly, MA) or Promega (Madison, WI). Resources and material procured to conduct the experiment are as follows: BMP2 and VEGF Enzyme-Linked Immunosorbent Assay kits, purchased from R&D Systems (Minneapolis, MN), the α4-integrin antibody, purchased from e-Biosciences (San Diego, CA); GFP antibody, purchased from Abcam (Cambridge, MA); and luciferase antibody, purchased from Chemicon (Billerica, MA).

Construction of plasmids and production of recombinant AAV2. All AAV2 plasmids were constructed using pSub201 as the backbone.[37] The complementary DNA-encoding rat BMP2 was kindly provided by Dr Chen (University of Texas at San Antonio, San Antonio, TX), and the complementary DNA-encoding mouse VEGF was excised from pBLAST49-mVEGF (InvivoGen, San Diego, CA). For bicistronic expression of BMP2 and VEGF, the coding sequence of BMP2 was cloned under cytomegalovirus promoter, and, VEGF sequence, following an internal ribosome entry site sequence downstream. The plasmid-encoding GFP has been described recently.[37] Packaging of rAAV6 was done in an adenovirus-free system as described.[37] Purification of the virions was done in a discontinuous iodixanol gradient centrifugation followed by heparin-affinity chromatography. Particle titers of the purified virions were determined by quantitative slot-blot analysis as described.[37]

Primary mouse MSC culture and gene transfer. Nude mice were purchased from the National Cancer Institute—Frederick Cancer Research Facility (Frederick, MD), and GFP transgenic mice [C57BL/6-Tg(ACTbEGFP)1Osb/J] were purchased from the Jackson Laboratories (Barr Harbor, ME). Luciferase-positive mouse MSC was purchased from Xenogen (Alameda, CA). All animal protocols were approved by the Institutional Animal Care and Use Committee. To obtain bone marrow-derived MSC, 4–6-week-old male mice were sacrificed; bone marrow was flushed from the femur and tibia; and the marrow mononuclear cells were purified by Ficoll gradient. Bone marrow stromal cells were grown in Stemline MSC expansion medium (Sigma, St Louis, MO) supplemented with 10% fetal bovine serum and 10^{-9} mol/l FGF2 to maintain the cells in pluripotent and undifferentiated state.[36] Residual macrophages from the MSC culture were removed by IMAC using antimouse CD11b beads (BD IMag; BD Biosciences, San Diego, CA). After 14 days, the adherent stromal

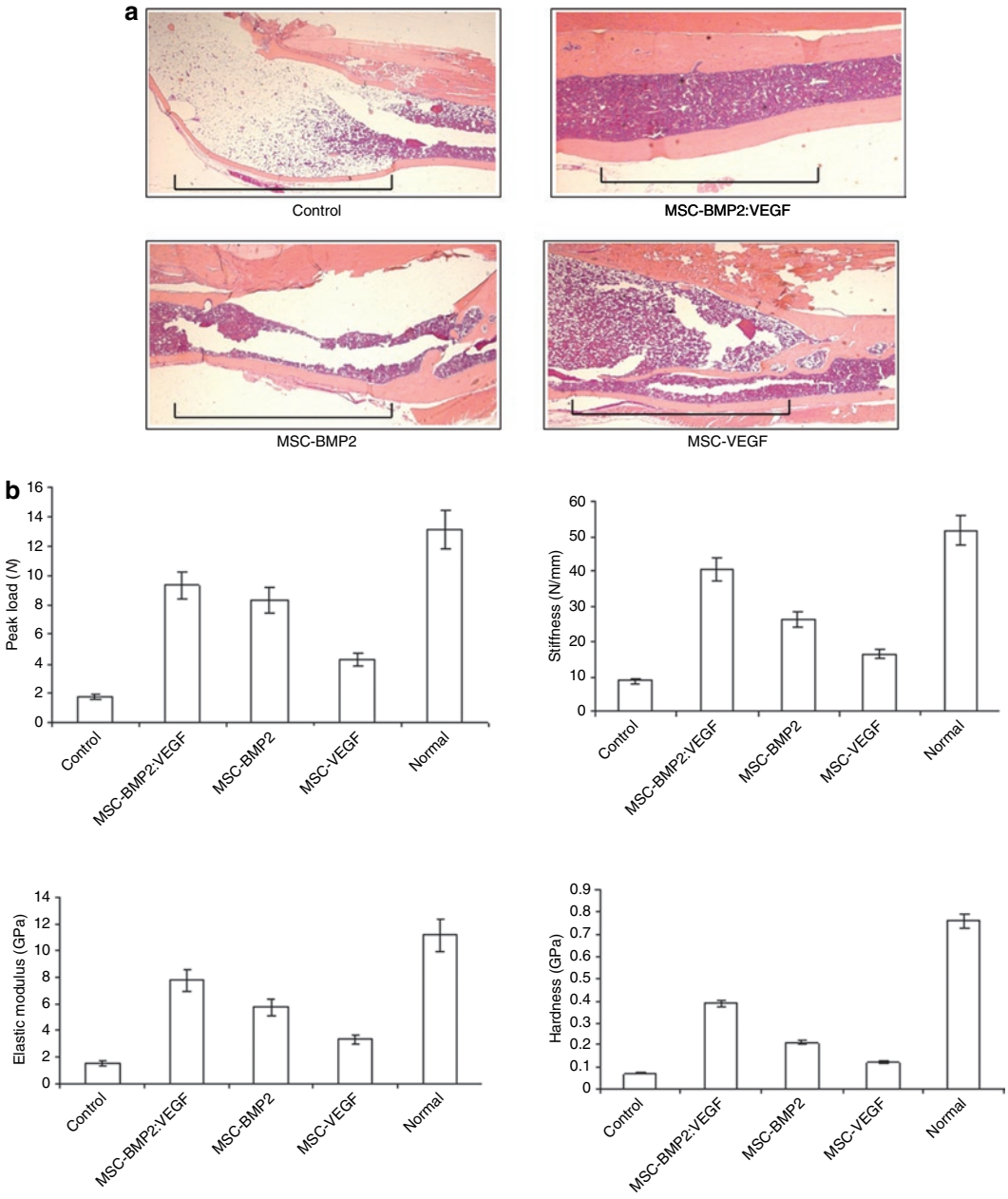

Figure 6 Osteogenic and angiogenic factors induce synergistic enhancement of bone healing in a segmental defect of tibia. (**a**) Histology of bone sections after H&E staining indicates significant increase of newly formed bone in the area of osteotomy, following treatment with MSC-expressing BMP2 and VEGF, compared to other groups. The region of segmental defect is indicated by horizontal lines in each panel. (**b**) Three-point bending tests (peak load, stiffness) and nanoindentation (elastic modulus and hardness) were performed on tibia isolated from the MSC-transplanted and control mice after 16 weeks of treatment. Data shown represent mean ± SD. $^*P < 0.05$. BMP2, bone morphogenetic protein 2; H&E, hematoxylin and eosin; MSC, mesenchymal stem cells; VEGF, vascular endothelial growth factor.

cells were split before attaining confluence to avoid possible onset of differentiation. The cells were routinely prepared and used for *in vitro* and *in vivo* studies as low-passage cultures (passages 4–8). Undifferentiated MSC were transduced with 1,000 multiplicity of infection (1 multiplicity of infection = 50 genomic particles) of rAAV6-BMP2:VEGF or rAAV6-GFP. Virus infection was performed in Opti-MEM for 2 hours at 37 °C following which complete medium with FGF2 was added. The cells were grown for ten more days before transplantation into mice.

Creation of segmental defect in tibia. Approximately 10–12-week-old athymic nude mice were used for creating segmental defects. Each animal was anesthetized with an isoflurane and oxygen mixture transferred onto a heating pad (maintained at 37 °C) in the operating field. Right tibiae of mice were fractured using a three-point bending apparatus and a 2–3-mm-long segmental defect was created. The fracture was stabilized with external pins and surgical sutures and tapes. Tylenol was added to drinking water as postoperative analgesia. Animals had free access to food and water and were monitored daily in the postoperative phase, to look for any complications or abnormal behavior.

Transplantation of MSC. A total of six mice were included in each group. Mock-transduced or rAAV6 (GFP or BMP2:VEGF)-transduced MSC were resuspended in a volume of 100 µl of normal saline and intravenously administered into recipient mice through tail vein. Before *in vivo*

administration, the cells were transiently transfected with the plasmid encoding the mouse α4-integrin. Cohorts of mice received a total of 1×10^6 MSC in five consecutive days (2×10^5 cells/injection) of untransduced, AAV6-GFP-transduced or AAV6-BMP2:VEGF-transduced MSC. Each week after transplantation, animals were subjected to DXA and after 16 weeks bones from each group were subjected to μCT analysis. Identification of homed MSC from the donor GFP mice was performed by GFP antibody staining, and luciferase MSC, by bioluminescence imaging.

Bioluminescent imaging. *In vivo* bioluminescence imaging was conducted in a cryogenically cooled IVIS-100 system (Xenogen) to detect luciferase expression in MSC using Living Image, an acquisition and analysis software (Xenogen). Briefly, mice were anesthetized with isoflurane and were intraperitoneally injected with 2.5-mg luciferin potassium salt (Xenogen) in phosphate-buffered saline. Imaging was performed after intravenous injection of luciferase-positive MSC. Image acquisition times were in the range of 10–240 seconds. The data acquisition software was calibrated to ensure that pixels remained saturated during image collection. Light emission from the tissue regions (relative photons/second) were measured using Living Image software (Xenogen). The intensity of light emission was represented with a pseudocolor scaling of bioluminescent images. The bioluminescent images superimposed on black-and-white images of mice were collected at the same time.

Quantification of BMP2 and VEGF levels in serum samples of transplanted animals. BMP2 and VEGF expressions in MSC, and in mouse serum, were collected from the animals at different time points and were determined using BMP2 and VEGF Quantikine kit Enzyme-Linked Immunosorbent Assay kits (R&D Systems), as per the manufacturer's instructions. A standard curve was generated using purified BMP2 and VEGF proteins to determine the concentrations of BMP2 and VEGF in serum.

DXA and μCT analyses of bone. For DXA analysis, animals were briefly anesthetized with isoflurane (2%)–oxygen mixture and placed in a prostrate position on the imaging plate. Bone mineral density, bone mineral content, and other body composition was assessed *in vivo* by DXA (GE-Lunar PIXImus, version 1.45; GE-Lunar, Madison, WI) periodically. To assess bone density, mass, geometry, and microarchitecture, intact tibia from each mouse was scanned using high-resolution μCT imaging system (μCT40; SCANCO Medical, Wayne, PA). Histomorphometric parameters, including bone volume, trabecular connectivity, trabecular thickness, trabecular separation, and degree of anisotropy, were evaluated.

Microfil perfusion and imaging of blood vessels. Cohorts of mice were sacrificed after 5 weeks to evaluate the blood-vessel formation. Mice were anesthetized with isoflurane, the thoracic cavity was opened surgically, and inferior vena cava was incised. The vasculature was flushed with normal saline containing heparin (100 U/ml) at a flow rate of 2 ml/minute via a needle inserted into the left ventricle. The specimens were then pressure-fixed with 10% buffered formalin. Formalin was flushed from the vessels in heparinized saline, and vasculature was injected with a radiopaque silicone rubber compound containing lead chromate (Microfil MV-122; Flow Tech, Carver, MA) solution prepared in a volume ratio of 4:5 of Microfil diluent with 5% curing agent. Samples were stored at 4 °C for contrast agent polymerization. Tibial bones were dissected and soaked for 48 hours in 10% buffered formalin to ensure complete tissue fixation. Tissues were subsequently treated in a formic acid-based solution, Cal-Ex II (Fisher Scientific, Pittsburgh, PA), to decalcify the bone and facilitate image thresholding of the vasculature from the surrounding tissues. Images were obtained using a high-resolution μCT imaging system (μCT 40; SCANCO Medical). Histomorphometric parameters, including vessel volume, connectivity, number, thickness, separation, and degree of anisotropy, were evaluated.

Biomechanical testing. All samples were fixed in formalin and stored in ethanol until mechanical testing. The bones were tested to failure by three-point bending on an 858 MiniBionix Materials Testing System (MTS Systems, Eden Prairie, MN). The samples were flexed at a rate of 0.03 mm/second with a support span of 10 mm for tibia with tension on the anteromedial surface. The load applicators were rollers of 2-mm diameter to avoid indenting the bone. Force–displacement data were plotted from which structural properties, including stiffness, peak load, and yield load, were obtained.[38] Stiffness was calculated as the slope of the linear portion of the load–displacement curve. Peak load and peak displacement were taken as the maximum load and displacement values attained during the test. Yield load was obtained by using a line drawn at 0.002 mm, parallel to the linear portion of the load–displacement curve. Toughness was measured as the area under the curve until fracture, whereas energy to yield was obtained as the area under the curve until yield.

Histology. Formalin-fixed tissues were decalcified in EDTA solution for 2 weeks and embedded in paraffin. Longitudinal sections of 5-μm thicknesses were cut from paraffin-embedded blocks of frontal sections of tibia, using a Leica 2265 microtome. Sections were then stained with hematoxylin and eosin for morphological examination.

Statistical analysis. All data are reported as mean ± SD. Bone mineral density and bone mineral contents were analyzed using analysis of variance. Comparison of differences between two variables was performed using the two-tailed, two-sample (with equal variances), independent *t*-tests. Results were considered significant at $P < 0.05$.

SUPPLEMENTARY MATERIAL

Figure S1a. Luciferase-positive MSC were transplanted intravenously and mice were sacrificed after 24 hours and lung, liver, spleen, heart, kidney, and adipose tissues were harvested.

Figure S1b. Microscopic identification of transplanted MSC in soft tissues.

Figure S1c. Quantitative analysis of luciferase expression in host tissues per microgram of protein.

Figure S2. Whole-body CT scan to visualize unintended ossification.

ACKNOWLEDGMENTS

Financial support of the National Institutes of Health Grant R01AR50251 and the U.S. Army Department of Defense Grants BC044440 and PC050949 are gratefully acknowledged.

REFERENCES

1. Praemer, A, Furner, S and Rice, DP (1999). *Musculoskeletal Conditions in the United States*. American Academy of Orthopaedic Surgeons: Rosemont.
2. Nolta, JA (ed.) (2006). *Gene Therapy for Mesenchymal Stem Cells*. Springer Science.
3. Franceschi, RT (2005). Biological approaches to bone regeneration by gene therapy. *J Dent Res* **84**: 1093–1103.
4. Ylä-Herttuala, S and Alitalo, K (2003). Gene transfer as a tool to induce therapeutic vascular growth. *Nat Med* **9**: 694–701.
5. Ferrara, N and Gerber, HP (2001). The role of vascular endothelial growth factor in angiogenesis. *Acta Haematol* **106**: 148–156.
6. Maes, C, Carmeliet, P, Moermans, K, Stockmans, I, Smets, N, Collen, D *et al.* (2002). Impaired angiogenesis and endochondral bone formation in mice lacking the vascular endothelial growth factor isoforms VEGF164 and VEGF188. *Mech Dev* **111**: 61–73.
7. Street, J, Bao, M, deGuzman, L, Bunting, S, Peale, FV Jr, Ferrara, N *et al.* (2002). Vascular endothelial growth factor stimulates bone repair by promoting angiogenesis and bone turnover. *Proc Natl Acad Sci USA* **99**: 9656–9661.
8. Gerber, HP, Vu, TH, Ryan, AM, Kowalski, J, Werb, Z and Ferrara, N (1999). VEGF couples hypertrophic cartilage remodeling, ossification and angiogenesis during endochondral bone formation. *Nat Med* **5**: 623–628.
9. Lieberman, JR and Friedlaender GE (2005). *Bone Regeneration and Repair Biology and Clinical Applications*. Gene Transfer Approaches to Enhancing Bone Healing. Humana Press.
10. Schmoekel, HG, Weber, FE, Schense, JC, Grätz, KW, Schawalder, P and Hubbell, JA (2005). Bone repair with a form of BMP-2 engineered for incorporation into fibrin cell ingrowth matrices. *Biotechnol Bioeng* **89**: 253–262.
11. Hashimoto, Y, Yoshida, G, Toyoda, H and Takaoka, K (2007). Generation of tendon-to-bone interface "enthesis" with use of recombinant BMP-2 in a rabbit model. *J Orthop Res* **25**: 1415–1424.
12. Fu, TS, Chen, WJ, Chen, LH, Lin, SS, Liu, SJ and Ueng, SW (2009). Enhancement of posterolateral lumbar spine fusion using low-dose rhBMP-2 and cultured marrow stromal cells. *J Orthop Res* **27**: 380–384.

13. Chang, SC, Chuang, H, Chen, YR, Yang, LC, Chen, JK, Mardini, S *et al.* (2004). Cranial repair using BMP-2 gene engineered bone marrow stromal cells. *J Surg Res* **119**: 85–91.
14. Baas, J, Elmengaard, B, Jensen, TB, Jakobsen, T, Andersen, NT and Soballe, K (2008). The effect of pretreating morselized allograft bone with rhBMP-2 and/or pamidronate on the fixation of porous Ti and HA-coated implants. *Biomaterials* **29**: 2915–2922.
15. Jiang, J, Fan, CY and Zeng, BF (2008). Osteogenic differentiation effects on rat bone marrow-derived mesenchymal stromal cells by lentivirus-mediated co-transfection of human BMP2 gene and VEGF165 gene. *Biotechnol Lett* **30**: 197–203.
16. Patel, ZS, Young, S, Tabata, Y, Jansen, JA, Wong, ME and Mikos, AG (2008). Dual delivery of an angiogenic and an osteogenic growth factor for bone regeneration in a critical size defect model. *Bone* **43**: 931–940.
17. Peng, H, Wright, V, Usas, A, Gearhart, B, Shen, HC, Cummins, J *et al.* (2002). Synergistic enhancement of bone formation and healing by stem cell-expressed VEGF and bone morphogenetic protein-4. *J Clin Invest* **110**: 751–759.
18. Richard, A, Carano, D and Filvaroff, EH (2003). Angiogenesis and bone repair. *Drug Discov Today* **8**: 980–989.
19. Kumar, S and Ponnazhagan, S (2007). Bone homing of mesenchymal stem cells by ectopic alpha 4 integrin expression. *FASEB J* **21**: 3917–3927.
20. Dimitriou, R, Tsiridis, E and Giannoudis, PV (2005). Current concepts of molecular aspects of bone healing. *Injury* **36**: 1392–1404.
21. Kumar, S, Nagy, TR and Ponnazhagan, S (2009). Therapeutic potential of genetically modified adult stem cells for osteopenia. *Gene Ther*; e-pub ahead of print 10 September 2009.
22. Byrne, AM, Bouchier-Hayes, DJ and Harmey, JH (2005). Angiogenic and cell survival functions of vascular endothelial growth factor (VEGF). *J Cell Mol Med* **9**: 777–794.
23. Dai, J and Rabie, AB (2007). VEGF: an essential mediator of both angiogenesis and endochondral ossification. *J Dent Res* **86**: 937–950.
24. Mayr-Wohlfart, U, Waltenberger, J, Hausser, H, Kessler, S, Günther, KP, Dehio, C *et al.* (2002). Vascular endothelial growth factor stimulates chemotactic migration of primary human osteoblasts. *Bone* **30**: 472–477.
25. Hsiong, SX and Mooney, DJ (2006). Regeneration of vascularized bone. *Periodontol 2000* **41**: 109–122.
26. Deckers, MM, Karperien, M, van der Bent, C, Yamashita, T, Papapoulos, SE and Löwik, CW (2000). Expression of vascular endothelial growth factors and their receptors during osteoblast differentiation. *Endocrinology* **141**: 1667–1674.
27. Midy, V and Plouët, J (1994). Vasculotropin/vascular endothelial growth factor induces differentiation in cultured osteoblasts. *Biochem Biophys Res Commun* **199**: 380–386.
28. Deckers, MM, van Bezooijen, RL, van der Horst, G, Hoogendam, J, van Der Bent, C, Papapoulos, SE *et al.* (2002). Bone morphogenetic proteins stimulate angiogenesis through osteoblast-derived vascular endothelial growth factor A. *Endocrinology* **143**: 1545–1553.
29. Raida, M, Heymann, AC, Günther, C and Niederwieser, D (2006). Role of bone morphogenetic protein 2 in the crosstalk between endothelial progenitor cells and mesenchymal stem cells. *Int J Mol Med* **18**: 735–739.
30. Dufourcq, P, Descamps, B, Tojais, NF, Leroux, L, Oses, P, Daret, D *et al.* (2008). Secreted frizzled-related protein-1 enhances mesenchymal stem cell function in angiogenesis and contributes to neovessel maturation. *Stem Cells* **26**: 2991–3001.
31. Krüger, M and Bechmann, I (2008). *Pericytes. Central Nervous System Diseases and Inflammation*. Biomedical and Life Sciences: Springer US.
32. Gerhardt, H and Betsholtz, C (2003). Endothelial-pericyte interactions in angiogenesis. *Cell Tissue Res* **314**: 15–23.
33. Bergers, G and Song, S (2005). The role of pericytes in blood-vessel formation and maintenance. *Neuro-oncology* **7**: 452–464.
34. Abramsson, A, Lindblom, P and Betsholtz, C (2003). Endothelial and nonendothelial sources of PDGF-B regulate pericyte recruitment and influence vascular pattern formation in tumors. *J Clin Invest* **112**: 1142–1151.
35. Bielby, R, Jones, E and McGonagle, D (2007). The role of mesenchymal stem cells in maintenance and repair of bone. *Injury* **38** Suppl 1: S26–S32.
36. Ren, C, Kumar, S, Shaw, DR and Ponnazhagan, S (2005). Genomic stability of self-complementary adeno-associated virus 2 during early stages of transduction in mouse muscle in vivo. *Hum Gene Ther* **16**: 1047–1057.
37. Kalajzcic, I, Kalajzcic, J, Hurley, M *et al.* (2003). Stage specific inhibition of osteoblast lineage differentiation by FGF2 and Noggin. *J Cell Biochem* **88**: 1168–1176.
38. Turner, CH and Burr, DB (1993). Basic biomechanical measurements of bone: a tutorial. *Bone* **14**: 595–608.